

AUTOMATIC CAMERA CALIBRATION IN CLOSE-RANGE PHOTOGRAMMETRY

Clive S. Fraser

CRC for Spatial Information
Dept. of Infrastructure Engineering
University of Melbourne
Victoria 3010 Australia
c.fraser@unimelb.edu.au

ABSTRACT

Automatic camera calibration via self-calibration with the aid of coded targets is now very much the norm in close-range photogrammetry. This is irrespective of whether the cameras to be calibrated are high-end metric, or the digital SLRs and consumer-grade models that are increasingly being employed for image-based 3D measurement. Automation has greatly simplified the calibration task, but there are real prospects that important camera calibration issues may be overlooked in what has become an almost black-box operation. This paper discusses the impact of a number of such issues, some of which relate to the functional model adopted for self-calibration, and others to practical aspects which need to be taken into account when pursuing optimal calibration accuracy and integrity. Issues discussed include interior orientation stability, calibration reliability, focal plane distortion, image point distribution, variation in lens distortion with image scale, colour imagery and chromatic aberration, and whether 3D object space control is warranted. By appreciating and accounting for these issues, users of automatic camera calibration will enhance the prospect of achieving an optimal recovery of scene-independent camera calibration parameters.

KEYWORDS: camera calibration, close-range, automation, self-calibration

INTRODUCTION

A useful starting point to the discussion on automated close-range camera calibration is consideration of the current state of the art. Nowadays, calibration - generally via the self-calibrating bundle adjustment technique - constitutes a standard, almost background operation in single-camera, off-line industrial and engineering photogrammetric measurement. The process can be considered in the same way as exterior orientation determination in multi-image networks, namely as a necessary recovery of nuisance parameters.

Having said that, it is certainly always true that the camera should have at some point been through a thorough initial calibration process, also fully automatic, which is designed to ascertain whether it meets the necessary metric requirements. For modern CCD or CMOS digital cameras with fixed focal length lenses, issues of metric quality centre mainly upon the degree of stability within the camera interior orientation parameters. High-end cameras especially built for industrial photogrammetry, such as the INCA3a from Geodetic Systems, can display angular resolutions of around 1 arc second after calibration, which translates to a 3D measurement accuracy capability of better than 1:100,000 of the size of the object in a 'strong' multi-image network. A root mean square value of image coordinate residuals (RMSE) ranging from 0.025 to 0.05 pixels is readily achievable in such calibrations, which indicates the high fidelity of the adopted functional model, as will be discussed in the next section.

Shown in Figure 1 is a typical photogrammetric network employed for automated close-range camera self-calibration. Characteristics of this network should be familiar: the many images, recorded at a fixed zoom/focus setting, with diversity in camera roll angles, are arranged in a strongly convergent imaging configuration. The 3D distribution of object points comprising both coded targets and supplementary single dots is photographed such that the resulting image points fill the focal plane in as many images as practicable. Given that the image measurement process is fully automatic, there is no reason not to incorporate significant observational redundancy in the process, and there are good reasons to do so, hence the use of generally a dozen images or more.

Given that automated close-range camera calibration can be conducted to such high accuracy and reliability, it is reasonable to ask why calibration is viewed as a vexing issue, especially in the computer vision community, as it has arguably been a largely solved problem in digital photogrammetry since automated exterior orientation determination came into practise in the early 1990s.

Unfortunately, the vast majority of cameras utilised today for moderate-accuracy close-range 3D measurement were not designed with photogrammetric accuracy in mind, so whereas it is certainly true that off-the-shelf digital cameras ranging from inexpensive consumer-grade to high-end prosumer-grade digital SLRs can be readily applied to photogrammetric measurement, their metric performance is generally well below the level that would be anticipated if the cameras were indeed fully ‘metric’. One could say that this is due to a shortcoming in calibration, but as this paper will endeavour to illustrate, it is not so much the process of automated calibration that is deficient, but the nature of the cameras and shortcomings in the imaging networks employed.

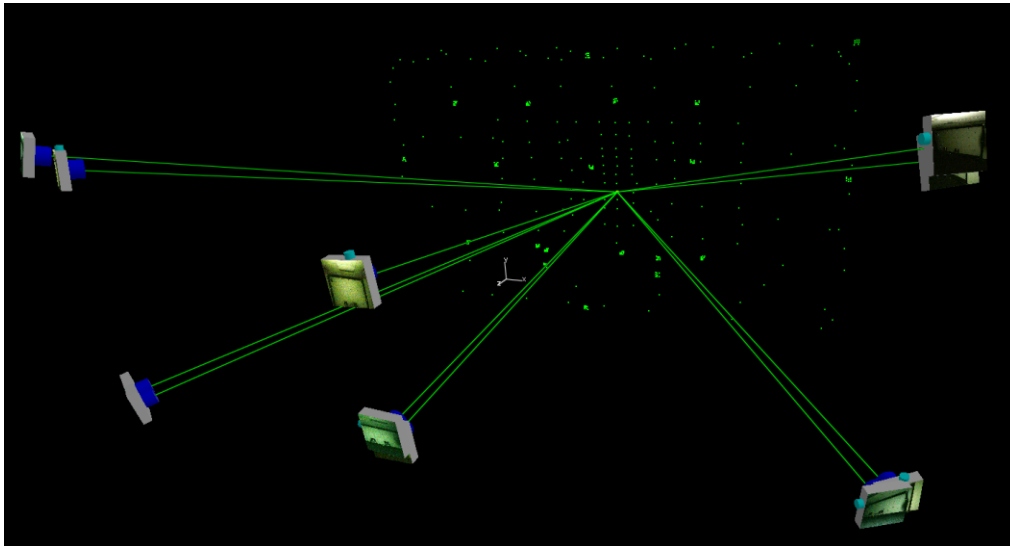


Figure 1. Representative network configuration for close-range camera self-calibration.

The purpose of this paper is to highlight the issues that can be expected to be confronted in the automatic calibration of cameras for close-range photogrammetry. The focus will be firmly upon ‘photogrammetric calibration’ which implies the generation of camera interior orientation and lens distortion parameters which are scene independent to the maximum extent possible, so that they will generally be applicable for the chosen camera settings. This goal is distinct from that which we often see in computer vision where the ‘calibration’ parameters are extracted from configurations involving minimal numbers of images and points, leading to high projective coupling between interior and exterior orientation parameters, the calibration then being only applicable to the network employed and not being viable for subsequent use requiring metric quality.

BRIEF REVIEW OF MATHEMATICAL MODEL

The mathematical basis of the self-calibrating bundle adjustment is the well-known extended collinearity model:

$$\begin{pmatrix} x - x_p + \Delta x \\ y - y_p + \Delta y \\ -c \end{pmatrix} = \lambda R \begin{pmatrix} X - X^C \\ Y - Y^C \\ Z - Z^C \end{pmatrix} \quad (1)$$

These equations describe the perspective transformation between the object space (object point X, Y, Z and perspective centre X^C, Y^C, Z^C with rotation matrix R) and image space (image point x, y). The calibration terms in Eq. 1 comprise the principal point offsets x_p, y_p and the principal distance c (the interior orientation parameters), and the image coordinate perturbation terms Δx and Δy which account for the departures from collinearity, or image distortion:

$$\begin{aligned}
x_p + \Delta x &= -\frac{\bar{x}}{c} \Delta c + \bar{x}r^2 K_1 + \bar{x}r^4 K_2 + \bar{x}r^6 K_3 + (2\bar{x}^2 + r^2)P_1 + 2P_2\bar{x}\bar{y} + b_1\bar{x} + b_2\bar{y} \\
y_p + \Delta y &= -\frac{\bar{y}}{c} \Delta c + \bar{y}r^2 K_1 + \bar{y}r^4 K_2 + \bar{y}r^6 K_3 + 2P_1\bar{x}\bar{y} + (2\bar{y}^2 + r^2)P_2
\end{aligned}
\tag{2}$$

where r is the radial distance to the image point:

$$r^2 = \bar{x}^2 + \bar{y}^2 = (x - x_0)^2 + (y - y_0)^2 \tag{3}$$

Within the self-calibration model, Eq. 2, Δc represents a correction to the initial principal distance value, K_i are the coefficients of radial distortion, P_i the coefficients of decentring distortion, and b_1 and b_2 are in-plane correction parameters for, respectively, differential scaling between the horizontal and vertical pixel spacings and non-orthogonality (axial skew) between the x and y axes.

CALIBRATION ISSUES

Within fully automatic camera calibration, there is an obvious temptation to simply adopt the full 10-parameter model of Eq. 2 as a default. Whereas this is indeed a practical approach in highly over-determined, geometrically strong self-calibration networks, it is not always the optimal approach. The reason is partially attributable to the role and significance of each of the parameters in the bundle adjustment, and to the intended use of the camera calibration. For example, it is well known that the decentring distortion parameters P_1 and P_2 are highly correlated with the principal point offsets x_p and y_p . Moreover, the decentring distortion correction is generally small, so that suppression of P_1 and P_2 in the self-calibration will typically see the error signal largely absorbed by x_p and y_p . This can be advantageous to users who are interfacing with photogrammetric image processing software that does not account for decentring distortion. A number of issues that face the user of automated metric calibration will now be considered. Some are practical in nature, whereas an appreciation of others may offer an insight into expected calibration outcomes in practise.

Interior Orientation Instability

Without a doubt, instability in camera interior orientation, be it instability between the image array and the housing; the lens and the camera body; and/or instability within the body or lens, is a major factor limiting the accuracy of multi-image close-range photogrammetric measurement. The calibration model of Eq. 2 is premised on the assumption of a stable interior orientation, and although extensions to this model have been employed to account for variable principal point offsets between images, such approaches generally do not lead to accuracy improvements. Also, they weaken the geometric strength of the self-calibration and go against the primary aim of producing a scene-independent calibration, applicable to all images recorded at a given zoom/focus setting. To quote from Augustine's Laws (Augustine, 1984) "If you want to make a silk purse out of a sow's ear, start with a silk pig" - the silk pig in this case being a camera with a highly stable interior orientation.

This is not to suggest that off-the-shelf consumer-grade digital cameras and prosumer-grade DSLRs cannot be usefully employed in close-range photogrammetry. Indeed they are, in increasingly larger numbers, with impressive results being obtained from inexpensive makes and models. But what it does suggest is that the metric limitations of such cameras need to be both recognised and quantified, and automatic calibration presents a very practical means for quantifying metric potential. Firstly, whereas one might expect an RMSE value of, say, 0.05 to 0.15 pixels for a digital SLR camera with a fixed focal length lens having minimal chromatic aberration, the equivalent value for a camera with integrated zoom, at a fixed focal setting, may well be 0.15 to 0.3 pixels, much of the difference being attributable to interior orientation instability.

Consider the results of two self-calibrations of a Nikon D200 with Nikkor 18-70mm zoom lens set to a nominal zoom focal length of 60 mm. The target field used was portable, approximately 66 x 66 cm with a depth of 11cm, and it comprised 54 x 3mm diameter retroreflective targets. This field was imaged in convergent networks comprising 18 camera stations. In the first calibration, the camera was immobile, stationary upon a tripod, and the target array was tilted and rotated to achieve the required image geometry. In the second calibration, the target array was stable and the camera was moved from station to station. No effort had been made to 'stabilise' the interior orientation, though the autofocus had been turned off. The resulting calibration parameters are shown in Table 1. The bundle adjustment with the stable camera produced an RMSE of 0.11 pixels and a mean standard error of object

point coordinates of 0.013mm (1:70,000 relative precision). Corresponding values for the freely moving camera (normal mode of operation) were 0.13 pixel and, again, 0.013mm, the convergence in the network with the stable target array being a little higher.

Table 1. Results obtained in two successive self-calibrations of the same camera/lens combination, in one case with the camera being in a fixed position and in the other with it being moved from station to station, as in normal operation. Δr and ΔP are the radial distortion and decentring profile values at 13mm radial distance.

	RMSE	c (mm)	x_p (mm)	y_p (mm)	Δr (μm)	ΔP (μm)
Camera stable, target array moved	0.70 μm (0.11 pixel)	59.21	-0.32	0.47	-144	24
Camera moved, target array stable	0.80 μm (0.13 pixel)	59.19	-0.25	0.26	-146	15

In Table 1 it can be seen that the repeatability of the parameter estimation is reasonably high for principal distance and radial lens distortion, as might be anticipated, but for principal point offset and decentring distortion, repeatability it is lower than would be desired, but again largely as anticipated. The ΔP value is from the decentring profile function and it quantifies the maximum tangential distortion component for a given radial distance. The discrepancies between the ΔP , x_p and y_p estimates are significant, especially when it is considered that sub-micrometre RMSE values are recovered in both calibrations. Moreover, when the triangulated object space coordinates are compared, the resulting RMS difference in coordinates is 0.03mm, which is higher than the 0.02mm that is predicted through error propagation. Nevertheless, the repeatability in object point coordinates is still impressive given that the x_p and y_p values differ by 0.07 and 0.21 mm, respectively.

What then do the results indicate? Firstly, it is clear that the increase in RMSE that accompanies normal (moving) operation of the camera is due to an apparent instability in the interior orientation. What is less clear is whether the variations in principal point offset and decentring distortion are due to projective coupling between the respective parameters, or to physical movements of lens elements, or a combination of the two. Both calibrations yield reasonable results, but can they be relied upon to the 1 μm model fidelity implied by the RMSE? In terms of object space coordinate determination, a reasonable degree of repeatability of calibration has been achieved, but this is not the case with four of the eight camera calibration parameters employed.

In this particular case, if the decentring parameters P_1 and P_2 are suppressed, the repeatability of the parameter x_p improves to 0.02mm, and y_p repeatability improves to 0.05mm. The question arises as to whether this is because these parameters are actually more stable and projective compensation is manifesting itself through absorption of the error signal by four parameters instead of two. Or, perhaps the lens is not stable, but the x_p and y_p parameters nevertheless absorb the decentring distortion effects as well. The focal length here could be regarded as 'long' in photogrammetric terms, the lens field of view being around 23°. As the field of view widens with smaller zoom focal length, the degree of projective coupling in a strong network can be expected to decrease and so a better modelling of both principal point coordinates and decentring distortion could be anticipated. But, in the presence of interior orientation instability, this does not necessarily assist with the goal of achieving a scene-independent calibration. There are basically only two courses of action available: (1) make a relatively modest effort to 'stiffen' up the body/lens connection through, for example, highly viscous lubricants and shims, or (2) accept the degradation in accuracy and reliability that is associated with interior orientation instability. Regrettably, when moving from strong multi-image convergent geometries to stereo or three-fold image coverage, it is not always a straightforward matter to quantify the impact of interior orientation instability.

Repeatability of Self-Calibration

Following on from the discussion of interior orientation instability, it is noteworthy that automatic self-calibrations take but 10 minutes or so to carry out. Thus, a recommended course of action is to record three or four networks of images and process all of them. The variation in camera parameters can then be examined, but the repeatability of the estimation of individual parameters is less important than the resulting differences in object space coordinates, since it is the integrity of the 3D measurement that is most important to the user. The repeatability in object space coordinate determination indicates the quality of the calibration, much more so than repeatability of individual camera calibration parameters, as has been illustrated by the example calibration summarised in the previous section.

In-plane and Out-of-plane Distortion

Throughout the era of film-based photogrammetry, the presence of out-of-plane distortion, as represented by film ‘unflatness’, constituted one of the major distinctions between metric and non-metric cameras. From research work on ‘additional parameter’ models for bundle adjustment in the 1980s, it became well recognised that the recovery of focal plane topography was not feasible with non-metric cameras and was generally less than satisfactory for metric cameras, even though empirical models found application. Also, it should be recalled that the influence of unflatness is most insidious in that it can invariably lead to significant accuracy degradation in object space coordinate determination in a bundle adjustment, without aggravating the magnitude of triangulation misclosures (RMSE values). With focal plane unflatness recovery in self-calibration largely being non-viable, and CCD and CMOS chips being small with specified tolerances on flatness, the net effect is that out-of-plane distortion is nowadays generally ignored. Experience to date with medium format CCD arrays suggests that the sensor surface may well exhibit a degree of planarity that does not warrant any unflatness correction. If there is a suspicion that focal plane flatness is a problem, then the only practical option is to utilise a lens of longer focal length; direct measurement of chip topography is no easy matter. When newer sensor technologies such as EMCCD, TFCCD and sCMOS (hybrid CCD and CMOS) become commonplace, and manufacturing technologies further improve with the ever-decreasing scalability of silicon technology, one can expect the effect of unflatness to become even less.

In the transition from film to digital cameras, there was a relatively brief flirtation with photogrammetric applications of video cameras. While the accuracy was poor, the prospects of real-time photogrammetric measurement were attractive. One of the calibration issues associated with video cameras was analog camera output and subsequent analog-to-digital image conversion, where frequency incompatibilities could result in in-plane distortion of the resulting image. The parameters b_1 and b_2 in Eq. 2 account for a scale variation between row and column pixel dimensions (pixel aspect ratio departing from 1) and a skewing of the image coordinate axes. This physical perturbation to the image has often been accommodated in projective models employed in computer vision by utilising two focal lengths, one each for the x and y axes, along with an axial skew coefficient.

Although video cameras have been superseded for metric applications for a decade or more, it is not uncommon for such parameterizations of in-plane distortion to persist, as exemplified by the popular Camera Calibration Toolbox for Matlab (http://www.vision.caltech.edu/bouguetj/calib_doc/). It is certainly reasonable to ask why! In the author’s experience, covering a hundred or more camera calibrations of modern consumer grade and digital SLR cameras, the affinity and non-orthogonality parameters have rarely been significant. While it is true that inclusion of b_1 and b_2 may well have a limited accuracy impact on geometrically strong self-calibration networks, their presence can nevertheless constitute over-parameterization in some cases. The resulting projective coupling with exterior orientation parameters, which is quantified through correlation coefficient values in the covariance matrix of parameters generated by the self-calibrating bundle adjustment, can give rise to distortions in the object point array. As a general recommendation, b_1 and b_2 should initially be suppressed, and then only included if there is an indication via an inflated RMSE value of the possible presence of in-plane distortion. If the subsequent inclusion of b_1 and b_2 into the self-calibration has no measurable impact upon the RMSE, then the parameters should again be suppressed.

One recent development in consumer-grade camera technology, which could potentially have an adverse impact on metric calibration, is in-camera distortion correction. Generally, software distortion correction is applied only to remove a proportion of obvious barrel distortion. However, in a recent self-calibration of a Fuji W1 stereo camera at three different zoom settings, it was found that at the widest angle setting the aspect ratio of the recorded image was adjusted such that the b_1 term was needed to model an introduced affinity which amounted to 22 pixels (37 μm) in x at the edge of the image format. Just why this affine distortion of the image is introduced, and only at the minimum zoom focal length, is not known, but it certainly impacts on metric performance. The RMSE in image space jumped from 0.2 pixels in a self-calibration at a mid-range zoom setting to 3.2 pixels at minimum zoom if the b_1 term was not employed. If the affinity term was employed, the RMSE fell to an acceptable 0.25 pixels. Just how users of a calibration including an affinity correction might utilise the correction in commercial photogrammetric software that does not accommodate it, is another issue. The implicit message here is to beware of undocumented in-camera ‘distortion correction’, which may not be able to be turned off. It should be turned off through the camera’s menu setting whenever possible.

Filling the Image Format

Radial lens distortion is modelled by an odd-order polynomial, up to degree 7, and while high-order polynomials are very effective interpolation functions, they are notoriously poor extrapolators. This well-recognised characteristic is too often ignored in camera calibration. Lens distortion needs to be described throughout the full image format, and thus image points must ‘fill the format’. It is not imperative to have formats of all images being fully covered, though it is desirable, but it is necessary to have all regions of the format out to the maximum radial

distance covered multiple times within the network of images. This also enhances recovery of camera interior orientation parameters as it helps to maximise the scale variation within convergent imagery.

Shown in Figure 2 are two plots of the radial lens distortion correction for the barrel distortion present in a Canon 17mm lens attached to a Canon EOS 20D DSLR camera. Both were obtained from the same 11-image, 300+ point self-calibration network, with the only distinction being that in one self-calibration, the maximum radial distance to any image point was 12.7mm (the maximum possible was 13.2mm) and in the other the corresponding value was 10.5mm. Thus, the correction plots beyond the respective vertical red lines in Fig. 2 are extrapolated. Note how the curves diverge, such that at the radial distance of 12.5mm, there is a 65 μ m or 10 pixel discrepancy between the Δr values obtained from image points at that radial distance and beyond, and those obtained via extrapolation. A 10 pixel error is very significant, and in this instance it is real. As lens focal length increases, one would expect this extrapolation error to decrease. Similarly, suppression of the K_3 coefficient from Eq. 2 might be expected to decrease the discrepancy, but omission of K_3 could well be inappropriate for wider-angle lenses such as the one considered here. As it happens, restricting the lens distortion model to cubic and fifth-order coefficients gives rise to a 13 μ m or 2 pixel Δr discrepancy at the same radial distance of 12.5mm.

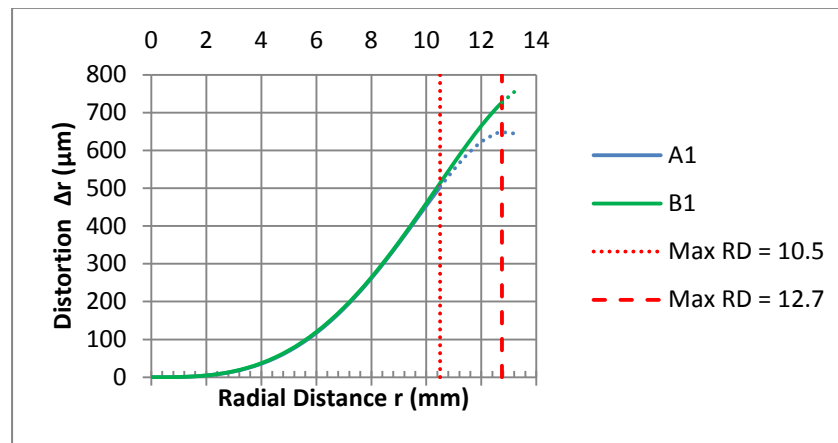


Figure 2. The problem of extrapolation of the radial distortion correction function beyond the largest radial distance (RD) to any image point. A1 and B1 are modelled distortion profiles corresponding to maximum encountered radial distances of 10.5mm and 12.7mm, respectively.

Alleviation of the lens distortion extrapolation problem is straightforward: fill the image format as much as possible. This not only enhances the integrity of any calibration term which is expressed as a function of radial distance, but it also renders unnecessary questions about whether to retain all of the K_i coefficients, or to suppress K_3 , and perhaps even K_2 , for narrow-angle lenses.

The Need for a 3D Object Point Array

The use of planar object point array, either portable or fixed, is not uncommon in close-range camera self-calibration. The adoption of highly convergent imaging configurations and orthogonal camera roll angles is sufficient to break the projective coupling between interior and exterior orientation parameters within the bundle adjustment. However, it is well recognised that adoption of a 3D object point array will enhance the accuracy of the recovered principal distance, and hence the adoption of rules of thumb such as depth variation within the target field of greater than 10% of the camera-to-object distance. From the days of analog stereo plotting of aerial photography, it has been known that errors in principal distance produce an affine distortion effect between planimetric (XY) and height (Z) coordinates. Yet, in close-range photogrammetry, we rarely hear reference to this distortion in object space, quite likely because self-calibration has become a normal operation and all object points are employed within the calibration process. The author recently encountered a case where affine distortion effects were clearly present and this particular case serves to illustrate the importance of adopting a 3D object point field for automatic camera calibration, at least if the camera is going to be applied over a large range of image scales.

Shown in Figure 3 is a photogrammetric network covering two ends of a 30m-long cylindrical object with a diameter of 5m. The aim of the measurement was to determine the circularity of each end of the cylinder (inner and outer surfaces), the relative alignment of the two end surfaces and the concentricity and length of the cylinder. Approximately 90 targets (including coded targets) were positioned on each end surface, with there being a further 16 back-to-back targets in the mid-section of the interior of the cylinder. This target array was imaged with a DSLR

camera with 24mm lens, from 7 camera stations at each end of the object, with four images being recorded at each camera station. The geometry of the camera stations was somewhat constrained by the need to image the targets within the cylinder as well as by other physical constraints in the building.

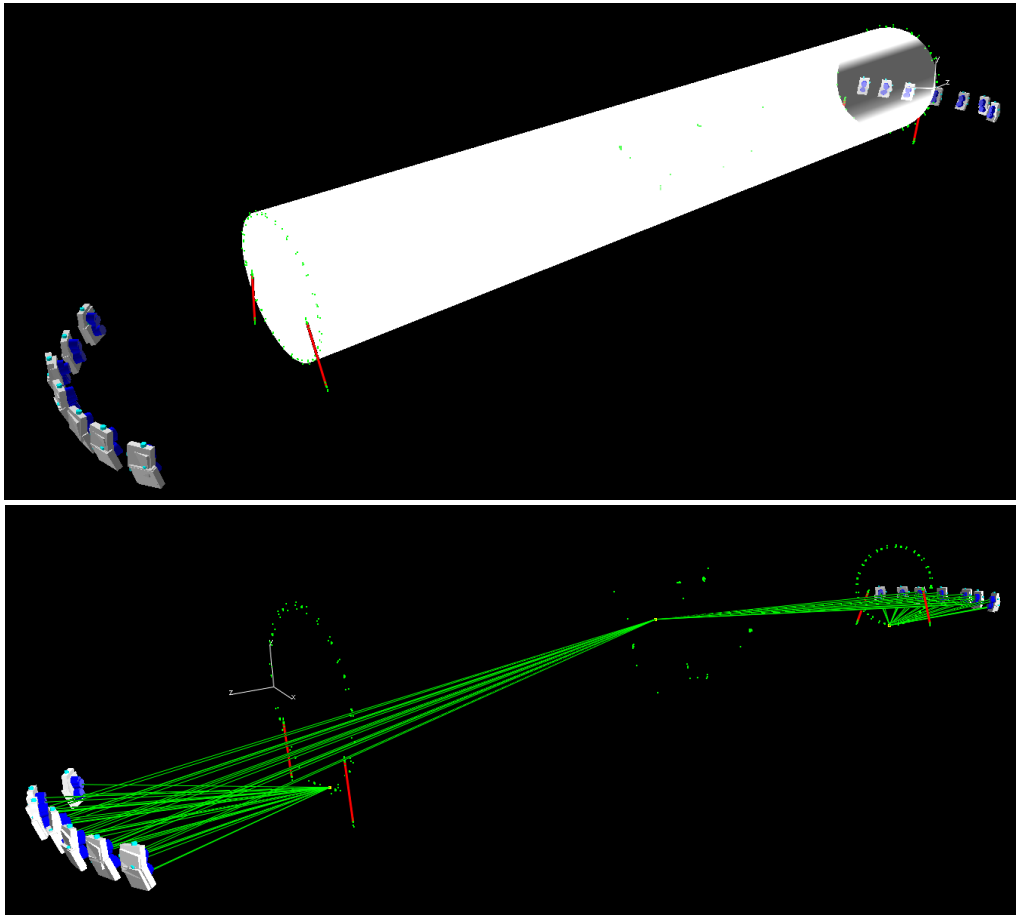


Figure 3. A 56-image network used to illustrate the affine scaling error than can arise from an error in principal distance.

The 56-image network was processed using a self-calibrating bundle adjustment and an RMSE value of 0.05 pixels was attained. The anticipated accuracy in object space coordinates was better than 0.01mm (RMS 1-sigma) for endpoints and up to 1.6mm (in the length direction) for mid points. The network was then scaled by four 1.6m long scale bars, two at each end. As is apparent from Figure 3, the self-calibration could be expected to be most influenced by the endpoint sub-networks, the intersection geometry of the midpoints being relatively weak. Thus, the principal distance could be said to have been determined from effectively two independent planar object point fields.

Based on the estimated object point accuracy, discrepancies in scale bar distances of the order of 0.15mm were anticipated and yet the values ranged from 0.4 to 0.6mm when all four bars were used. Moreover, if only the two scale bars at one end were used, the discrepancies reduced to less than 0.05mm on these distances, but increased to 1mm on the two bars at the other end, 1.1mm for one pair, and -1.1mm on the other. This implied an affine distortion of 22mm over the 30m length of the cylinder, or 1 part in 1400. A change in principal distance of only 0.017mm would account for such a differential scale error. The bundle adjustment was re-run, with a fixed principal distance 17 μ m shorter than in the initial self-calibration. The net effect of this was that the RMSE value changed by only 0.01 μ m, yet the four scale bar distances all agreed to better than 0.05mm. Without the small principal distance correction, the cylinder length determination was in error by 89mm. Incorporation of depth in the object point array – but not depth as is represented in this example – can alleviate the affine scaling error. The potential for its presence also partially explains the often heard observation that photogrammetry is “not at its best when measuring long, thin objects”. When in doubt, simply add target points so as to realise a 3D point distribution in the self-calibration network.

The Provision of Control Points

One of the merits of fully automatic camera self-calibration is that it can be carried out without the need for an object point array of accurately known 3D coordinates. Indeed no prior information on target positions is needed and nor is object space scale. If required, nominally true scale can generally be set from knowledge of the coded target size. The question then arises as to whether the provision of independently surveyed coordinate data for the points forming the target field is useful, and the answer has to be: *not really*. Where object point coordinates are known it can be reassuring to quantify the quality of the calibration through an accuracy check of triangulated object points against the control points, but with very strong network geometry, one can expect this to yield little further information than is gained via checks between multiple independent calibrations. A good deal of expense in cost and time is involved in setting up and maintaining surveyed control point arrays, and it is reassuring to know that they are not needed for automated camera calibration.

Distortion Variation with Focus and Zoom

Camera calibration parameters, and especially those related to lens distortion, vary significantly with zoom and focus setting. Mathematical models have been formulated to describe the variation of radial lens distortion with focus (Brown, 1971) and there has been a recent development, called zoom-dependent (Z-D) calibration (Fraser & Al Ajlouni, 2006) which models the variation of lens distortion with zoom setting, thus removing the necessity for the camera zoom setting to be fixed and stable during the image capture process. Nevertheless, recording images with a fixed zoom and focus setting remains the universal practise within close-range photogrammetry. There may well be more than a single zoom/focus setting employed in a single image network, but there needs to be (a) a calibration for each setting, or (b) a geometric arrangement that supports the simultaneous self-calibration for all settings. The topic of variation of lens distortion, which needs only to consider radial and not decentring distortion for practical purposes, will not be further considered in this paper, as it does not constitute an issue of concern. Instead, the user generally needs to ensure that once the zoom and focus settings are set, they remain at those settings, and this consideration forms part of the process of ensuring physical stability of the camera interior orientation. What is reassuring in the context of automatic camera calibration, is that it is a simple matter to recover the calibration parameters for the chosen zoom and focus settings.

Colour Images

While it is recognised that monochrome digital cameras have accuracy advantages over colour cameras, the issue is nowadays essentially moot, because virtually all consumer-grade through to professional digital cameras incorporate colour filter arrays whereby only one colour is recorded at each pixel location. Most commonly it will be red, green or blue as a consequence of the widely used Bayer Pattern filter array. However, it could also be, for example, cyan, magenta, yellow and green. There are basically two factors limiting photogrammetric accuracy of colour cameras, as compared to their Black and White equivalents. The first is the metric impact of the in-camera pre-processing that is carried to convert a 10-, 12-, 14- or 16-bit recorded RAW image to a more common 8-bit format such as JPEG, which is required for displaying on a computer screen. The second factor is chromatic aberration.

Within an image recorded using a Bayer Pattern filter array, half the pixels are green, whereas red and blue pixels each comprise 25% of the total. The demosaicing operation required to produce full RGB colours for each pixel, each in a separate channel, involves interpolation and thus an inherent loss of spatial resolution of the sensor. Further adverse metric impacts, though admittedly small, can arise through other RGB image creation processes such as noise reduction, white-balance correction, gamma shifting, image sharpening and most significantly, image compression (Stamatopoulos, 2011). From a practical standpoint there is little that the user can do about these influences in the context of camera calibration, other than acknowledging their presence. Thus, they are generally ignored. Attention is of course given to acquisition of imagery with the optimal radiometric quality for a particular application. In the typical case where the image file format is JPEG, it is advisable to keep the compression ratio to a modest level of 10% or more.

Chromatic Aberration

In terms of the accuracy spoken of previously as being achievable with automatic camera self-calibration, RMSE values of around 0.05 to 0.1 pixels can be generally anticipated for digital SLR cameras with fixed focal length cameras, whereas 0.1 – 0.3 pixels is more representative for less expensive cameras with integrated zoom lenses. Such calibration accuracy is certainly adequate for a host of measurement applications, many of which require colour imagery for the final photogrammetric product, eg colour orthomosaics or 3D textured models. One of the photogrammetric concerns of RGB imagery centres upon chromatic aberration within the lens, the metric

impact of which can be that each colour channel will have a distinct principal distance and radial lens distortion profile. The effect of chromatic aberration can be seen when examining a zoomed-in section of a typical colour image containing a traditional white-on-black photogrammetric target. The image of the target will appear to be 'smeared', mainly in a radial direction, with the 'red-ish' pixels smeared in the opposite direction to 'blue-ish' pixels, and the 'green-ish' pixels left in focus at the centre of the target (in the typical case where the lens is set for optimal focus of green light). The effect becomes more pronounced with increasing radial distance.

The presence of variations between principal distance and radial lens distortion coefficient values for the R, G and B channels constitutes a possible source of error for camera self-calibration and studies (Cronk et al., 2006; Luhmann et al., 2006) have indicated that whereas the metric impact is unlikely to be significant in the calibration of consumer grade cameras, it can certainly limit the attainable accuracy of higher-end DSLR cameras. For these sensors, the resulting error in the centroiding of targets within the imagery can be mitigated either by considering different calibration parameters (c and K_i terms) for each colour channel, with associated constraints on exterior orientation (Luhmann et al., 2006), or by pre-processing the imagery to model the effects of chromatic aberration and then considering the three colour bands as normal. Either method requires access to the raw camera imagery, which contains the original and separate R, G and B information. A very practical means to minimize the metric impact is to seek out a lens which displays very little chromatic aberration. Recent investigations have indicated that whereas the RMS discrepancy value between centroids determined for the R and G, and G and B channels for points distributed throughout the image format of commonly used 20mm and 24mm fixed focal length lenses is generally at the level of $1/20^{\text{th}}$ of a pixel, with individual differences near the edge of the image format being as high as several pixels, the overall degradation within the accuracy of object point determination is modest. Thus, the effect of chromatic aberration is generally acknowledged but not specifically accounted for in camera calibration.

CONCLUDING REMARKS

The aim of this paper has been to review a number of issues which impact upon the quality and integrity of automatic close range camera calibration via the self-calibrating bundle adjustment, and thus provide an insight into some of the less-appreciated aspects of the calibration process. Beyond emphasising the fact that interior orientation instability inherent in off-the-shelf digital cameras poses the major limiting factor to the quality of calibration, at least in the sense of recovery of stable, scene independent camera parameters, this account has also touched upon the make-up of the additional parameter model, and also upon aspects of the image formation process and photogrammetric network geometry. Most of these are well recognised by photogrammetrists, but there's a tendency for users to assume that automatic camera calibration via self-calibration, as a black-box operation at least, will always yield the desired calibration reliability and accuracy. Whereas there are necessary, basic rules for close-range camera self-calibration, these may not always be sufficient to yield the desired results. It is hoped that this account will have provided useful insights into the main issues which impact upon automatic camera calibration for close-range photogrammetry.

REFERENCES

- Augustine, N.R., 1984. *Augustine's Laws*. AIAA, 6th Edition, 1997, 395 pages, ISBN-13: 978-1-56347-240-4.
- Brown, D.C., 1971. Close-Range Camera Calibration. *Photogrammetric Engineering*, 37(8): 855-866.
- Cronk, S., Fraser, C.S. and Hanley, H.B., 2006. Automatic Calibration of Colour Digital Cameras. *Photogrammetric Record*, 21(116): 355-372.
- Fraser, C.S. and Al-Ajlouni, S., 2006. Zoom-Dependent Camera Calibration in Close-Range Photogrammetry. *Photogrammetric Engineering & Remote Sensing*, 72(9): 1017-1026.
- Luhmann, T., Hastedt, H., Tecklenburg, W., 2006. Modelling of Chromatic Aberration for High Precision Photogrammetry. *International Archives of Photogrammetry, Remote Sensing and Spatial Information Sciences*, Vol XXXVI, Part5: 173-178.
- Stamatopoulos, C., 2011. *Orientation and Calibration of Long Focal Length Cameras in Digital Close-Range Photogrammetry*. PhD Thesis, Dept. of Infrastructure Engineering, University of Melbourne, 170 pages.